frontiers in Chemistry

ORIGINAL RESEARCH
published: 25 June 2021
doi: 10.3389/fchem.2021.704012

A Robust Recovery of Ni From Laterite Ore Promoted by Sodium Thiosulfate Through Hydrogen-Thermal Reduction

Shoujun Liu[1,2,3], *Chao Yang*[2,3], *Song Yang*[1,2]*, *Zhongliang Yu*[2,4]*, *Zhao Wang*[1,2], *Kang Yan*[1,2], *Jin Li*[2,5] *and Xingyang Liu*[1,2]

[1]College of Chemistry and Chemical Engineering, Taiyuan University of Technology, Taiyuan, China, [2]Shanxi Engineering Center of Civil Clean Fuel, Taiyuan University of Technology, Taiyuan, China, [3]Key Laboratory for Coal Science and Technology of Ministry of Education and Shanxi Province, Taiyuan University of Technology, Taiyuan, China, [4]School of Chemistry and Environmental Science, Shangrao Normal University, Shangrao, China, [5]Taiyuan Green Coke Energy Co. Ltd., Taiyuan, China

OPEN ACCESS

Edited by:
Kai Yan,
Sun Yat-Sen University, China

Reviewed by:
Zhaohui Chen,
Polytechnique Montréal, Canada
Zhanggen Huang,
Institute of Coal Chemistry, Chinese Academy of Sciences, China
Qingya Liu,
Beijing University of Chemical Technology, China

***Correspondence:**
Song Yang
yangsong@tyut.edu.cn
Zhongliang Yu
yzh2401@126.com

Specialty section:
This article was submitted to Green and Sustainable Chemistry, a section of the journal Frontiers in Chemistry

Received: *01 May 2021*
Accepted: *14 June 2021*
Published: *25 June 2021*

Citation:
Liu S, Yang C, Yang S, Yu Z, Wang Z, Yan K, Li J and Liu X (2021) A Robust Recovery of Ni From Laterite Ore Promoted by Sodium Thiosulfate Through Hydrogen-Thermal Reduction. Front. Chem. 9:704012. doi: 10.3389/fchem.2021.704012

Laterite ore is one of the important sources of nickel (Ni). However, it is difficult to liberate Ni from ore structure during reduction roasting. This paper provided an effective way for a robust recovery of Ni from laterite ore by H_2 reduction using sodium thiosulfate ($Na_2S_2O_3$) as a promoter. . It was found that a Ni content of 9.97% and a Ni recovery of 99.24% were achieved with 20 wt% $Na_2S_2O_3$ at 1,100°C. The promoting mechanism of $Na_2S_2O_3$ in laterite ore reduction by H_2 was also investigated. The thermogravimetric results suggested the formation of $Na_2Mg_2SiO_7$, Na_2SO_3, Na_2SO_4, and S during the pyrolysis of laterite with $Na_2S_2O_3$, among which the alkali metal salts could destroy the structures of nickel-bearing silicate minerals and hence release Ni, while S could participate in the formation of the low-melting-point eutectic phase of FeS-Fe. The formation of low-melting-point phases were further verified by the morphology analysis, which could improve the aggregation of Ni-Fe particles due to the capillary forces of FeS-Fe as well as the enhanced element migration by the liquid phase of sodium silicates during reduction.

Keywords: laterite ore, sodium thiosulfate, hydrogen reduction, ferronickel, magnetic separation, mechanism

INTRODUCTION

Nickel, as a ferromagnetic metal with a high corrosion resistance, plasticity, and magnetism, has been intensively used in many applications involving nickel-based alloys and stainless steel as well as in fuel cells (Sudagar et al., 2013). Stainless steel production accounts for 65% of the global nickel consumption (Moskalyk and Alfantazi, 2002). Sulfide ore and nickel laterite ore are the two main commercial nickel resources. With the gradual decline of sulfide ores deposits, nickel laterite ores are playing more important roles than before with the growth of worldwide nickel output (Quast et al., 2015a). Therefore, it is great meaningful to recover Ni effectively from nickel laterite ores from the viewpoint of sustainable development.

Nickel laterite ores can be divided into two different types, namely saprolitic and limonitic ores, based on the chemical and physical characteristics (Hidayat et al., 2008). As reported Katzagiannakis et al. (2014); Khataee et al. (2015), the laterite cannot be easily used through physical methods because of its poor crystallinity and fine grains. Zhu et al. (2012a) investigated the mineralogy and crystal chemistry of a low-grade limonite-type nickel laterite ore and found that the Ni was mainly present in the goethite and silicates

phases. Therefore, it is required to eliminate the restriction of the goethite and silicates phases first for the Ni liberation, which can then be beneficiated by subsequent treatment technology, such as reduction roasting followed by magnetic separation (Zhu et al., 2012b).

Recently, several researchers have focused on the reduction roasting of laterite ore with different reductants such as carbon, CO or H_2, followed by magnetic separation (Lu et al., 2013; Quast et al., 2015b). In addition, compared with C and CO, hydrogen has a good carbon footprint, and the carbon footprint is relatively stable, close to zero, which is conducive to better carbon neutralization. (Valente et al., 2020). In recent years, a number of studies (Hu et al., 2019; Zhang et al., 2020) have focused on the selective conversion of biomass into renewable energy, such as hydrogen, As a reducing agent, hydrogen has strong environmental benefits. Moreover, the additives, such as Na_2CO_3, S, NaCl, and Na_2SO_4, have been used to enhance the enrichment ratio of Ni (Li et al., 2012; Jiang et al., 2013). Oliveira V D A et al. (de Alvarenga Oliveira et al., 2020) studied the reduction kinetics of limonite under the action of hydrogen and found that the diffusion of reagent (H_2) or product (gaseous H_2O) through the ash layer is a slow process step. Harris et al. (2011) selected sulfur (S_2) as the additive for the laterite ores calcination at 450, 500, and 550°C and observed that the nickel extraction and selectivity were improved by the increasing temperature. Li et al. (2012) studied the beneficiation of nickeliferous laterite by reduction roasting in the presence of sodium sulfate and noticed when the laterite was mixed with sodium sulfate and then reduced at 1,100°C for 60 min, the Ni grade of the concentrate and recovery were increased to 9.48 and 83.01%, respectively. Lu et al. (2013) investigated the effect of sodium sulfate on the hydrogen reduction process of nickel laterite ore. In conclusion, the alkali metal additives can be used to improve the reactivity of reducing agents, and to break the structure of Ni-containing silicate. While the sulfur additives are usually applied to improve the grade of Ni. Based on the discuss above, it is more excepted to find an green and cheap additive that could play the dual roles of alkali metals and sulfur compounds at the same time, because this could not only remarkably decrease the operation cost, but also alleviate the environmental pollution.

Sodium thiosulfate is a common raw chemical material that can provide alkali metals and elemental sulfur simultaneously. Mcamish and Johnston (1976) analyzed the sulfur exchange and decomposition kinetics in solid $Na_2S_2O_3$ and found that the decomposition of $Na_2S_2O_3$ occurred in a temperature range from 290 to 350°C, with the main products of S, Na_2S and Na_2SO_4. However, limited studies on this topic have been reported, especially the effect and mechanism of sodium thiosulfate on promoting the laterite ore reduction.

Therefore, in current study, sodium thiosulfate was employed to improve the grade and recovery of nickel by hydrogen reduction of laterite followed by magnetic separation. The effects of temperature, reduction time, and sodium thiosulfate on the nickel laterite reduction were investigated. The samples were characterized in detail by inductively coupled plasma-atomic emission spectrometry (ICP-AES), X-ray diffraction analysis (XRD), and scanning electron microscopy coupled with an energy dispersive X-ray spectroscopy (SEM-EDS). Based on the collected data, the promotion mechanism of sodium thiosulfate for hydrogen-thermal reduction of laterite ore was proposed.

EXPERIMENTAL

Materials

Nickel laterite ore from Indonesia was used as the raw ore, which is Limonitic Nickel Ore. Reagent grade sodium thiosulfate ($Na_2S_2O_3$), purchased from Tianjin Kemiou Chemical Reagent Co., Ltd., China, was selected as the additive. Hydrogen (99.99 vol %) was employed as the gaseous reductant. Nitrogen (99.99 vol%) was employed as the protective and balance gas. All the gases were supplied by Taiyuan iron and steel Co., Ltd.

Sample Preparation

The samples were prepared as follows. First, the as-received nickel laterite ore was air-dried at 105°C overnight in an oven. Second, the dried nickel laterite ore was crushed to a particle size of less than 2 mm using a jaw crusher. After, the crushed nickel laterite ore was ground using a laboratory-scale ball mill and was subsequently sieved to a particle size of less than 80 mesh. Finally, the raw ore and $Na_2S_2O_3$ are ground with a sample maker, then sieved with a 100–140 mesh sieve, and finally mixed in a beaker, the $Na_2S_2O_3$ contents of 5, 10, 15, 20 or 25 wt%. The corresponding nickel laterite ores with different contents of sodium thiosulfate were denoted as prepared ore (PO).

Reduction Experiments and Magnetic Separation Process

A typical reduction experiment of PO was conducted as follows. Approximately 80 g of PO loaded into a stirred fixed-bed reactor (Lu et al., 2013). The temperature of the PO during roasting and reduction roasting with H_2 was monitored by a thermocouple inserted into the reactor. Then PO was heated at 450°C for 1 h under a nitrogen atmosphere (0.7 L/min). Thereafter, the reactor was heated to the final reaction temperature, and then 27 L/min of H_2/N_2 (45/55) was introduced to reduce the ores. After the reduction process was complete, the ore samples were cooled to room temperature under a nitrogen atmosphere (0.1 L/min). The effects of the reduction temperature, time, and the dosage of $Na_2S_2O_3$ were investigated.

After reduction, 5 g of product was ground to a particle size of 90 wt % passing 0.043 mm using a rod mill. These particles were then separated in a Magnetic Tube (XCGS-73 Davies) with a magnetic field intensity of 0.1 T to obtain the Fe-Ni concentrates. The grade of Ni in sample were determined by chemical analysis of dimethylglyoxime photometry., and the grade of Fe were determined by the potassium dichromate method. The recovery rate of Ni was calculated according to the following equation (Lu et al., 2013):

$$R_{Ni/Fe} = m_1/m_2 \times 100\% \quad (1)$$

where $R_{Ni/Fe}$ is the nickel or iron recovery rate, and m_1 and m_2 are the elemental nickel or iron contents in the concentrate and the reduced samples, respectively.

Analysis and Characterization

The main chemical composition of nickel laterite ore and the contents of Fe and Ni in each sample were determined by inductively coupled plasma atomic emission spectrometry (ICP-AES-9000(N + M), a commercial product of Thermo

TABLE 1 | Main chemical composition of nickel laterite ore (wt%).

TFe	TNi	Al_2O_3	CaO	MgO	Cr_2O_3	SiO_2	P_2O_5	MnO_2	Co
24.14	1.41	3.15	1.46	14.58	1.08	29.36	0.018	1.46	0.065

Jarrell-Ash Corp., United States. The distribution of nickel in the laterite was analyzed by chemical phase analysis, as reported previously (Mcamish and Johnston, 1976).

The crystalline phases of the samples were recorded using an X-ray diffractometer (Rigaku D/Max 2,500, Japan) under the following conditions: Cu-Kα radiation of 150 mA and a scanning rate of 3°/min from 5 to 85°. The morphological changes were analyzed by scanning electron microscopy with an energy dispersive X-ray spectroscopy (SEM-EDS) (Phenom ProX, Netherlands).

A Setaram SETSYS TGA was used to study the weight loss during the decomposition of laterite ore blended with $Na_2S_2O_3$. Approximately 25 mg of mixture was heated under 100 ml/min of Ar flow with a ramp rate of 10°C/min from room temperature to 1,050°C. The obtained TG data was further processed to determine the net weight loss for the decomposition analysis using the following equation:

$$W_L = (m - m_T)/(m - m_{1050}) \times 100\% \quad (2)$$

where W_L is the net weight loss; m_T is the mass of the sample at the temperature of T; m_{1050} is the mass of the sample at 1050°C; and m is the initial mass of sample.

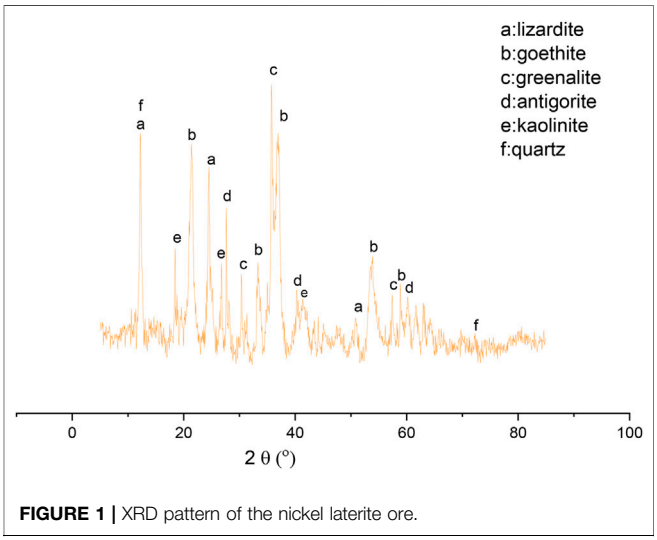

FIGURE 1 | XRD pattern of the nickel laterite ore.

TABLE 2 | Nickel distribution state of the studied laterite.

Type	Silicates	Oxides	Sulphides	Adsorption	Ni_{total}
Contents/wt%	1.19	0.12	0.07	0.03	1.41
Ratio/%	84.40	8.51	4.96	2.13	100

RESULT AND DISCUSSION

Characterization of Raw Nickel Laterite Ore

Table 1 shows the main chemical composition of the raw nickel laterite, which contained 1.41 wt% of Ni, 24.14 wt% of Fe, 3.15 wt% of Al_2O_3, 1.46 wt% of CaO, 14.58 wt% of MgO, 29.36 wt% of SiO_2, 0.018 wt% of P_2O_5, 1.46 wt% of MnO_2, and 0.065 wt% of Co. Valix and Cheung (2002) investigated the mineralogical properties of nickel laterite and found that the element content ranges of limonitic nickel ore was Ni 1.5–1.8 wt%, Fe 25–40 wt%, Co 0.02–0.1 wt%, MgO 5–15 wt%, and Cr_2O_3 1-2 wt%.

Table II. Measured and Theoretically Calculated Mass Losses as wel.

Figure 1 shows the XRD patterns of the raw nickel laterite ore. The raw laterite ore mainly consisted of lizardite, goethite, greenalite, antigorite, kaolinite, and quartz. However, no nickel-containing phases were evident in the XRD patterns, which may be due to the low nickel content or the poor crystallinity of the nickel phase in the raw laterite ore (Zeissink, 1969). This indicated that the nickel laterite ore used in this study was a typical transition layer laterite ore.

To understand the nickel form in the laterite ore, the nickel distribution state of the studied laterite was examined by chemical titration, as shown in **Table 2**. The nickel mainly existed as the silicate minerals, which accounted for 84.4% of the total nickel, followed by the oxide minerals (8.51%), the sulphides minerals (4.96%), and the adsorption minerals.

Because some magnesium ions contained in the serpentine could exchange Ni ions during the weathering of laterite ore, the nickel enrichment process in serpentine olivine and other silicates ores can be expressed as follows (Kim et al., 2010):

$$\text{Mg serpentine} + Ni^{2+} \rightarrow \text{Ni serpentine} + Mg^{2+} \quad (3)$$

Therefore, the breakage of the nickel-rich sillicate structures is the key step for improving the nickel recovery by calcination.

Effects of Different Reduction Conditions on Ni Beneficiation

Effect of Sodium Thiosulfate Dosage on Ni and Fe Beneficiation

The Ni grade and recovery of laterite reduced with varied dosages of $Na_2S_2O_3$ (ranging between 0 and 25 wt%) are displayed in **Figure 2**. As shown in **Figure 2A**, without $Na_2S_2O_3$, the nickel grade and recovery only reached 1.65 and 50.34%, respectively. However, with 25 wt% $Na_2S_2O_3$, the nickel grade and recovery were improved to 9.53 and 97.73%, respectively. With the increase in the $Na_2S_2O_3$ addition, the nickel grade and recovery were increased as well. However, the iron grade was only slightly improved, and the iron recovery decreased

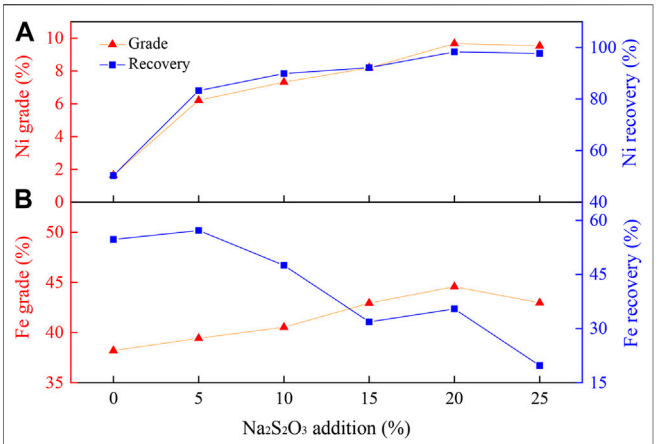

FIGURE 2 | | Effect of $Na_2S_2O_3$ addition on the **(A)** nickel and **(B)** iron enrichment.

significantly with the increase in $Na_2S_2O_3$ (**Figure 2B**). This shows that the addition of $Na_2S_2O_3$ was not only conducive to the improvement of the nickel grade but also had a significant effect on the iron removal, which could then achieve the selective recovery of nickel and iron. When the addition of $Na_2S_2O_3$ exceeded 20 wt%, both the grade and recovery of nickel and iron were only slightly changed compare to the result with the $Na_2S_2O_3$ of 25 wt%. Hence, based on the cost and quality of the nickel concentrate, a 20 wt% addition of $Na_2S_2O_3$ was chosen for the following experiments.

Experimental conditions: temperature, 1000°C; reduction time, 90 min; flow rate of H_2/N_2, 27 L/(min kg); gas volume fraction of H_2, 45 vol%; grinding fineness, 85 wt% passing 0.074 mm; magnetic field intensity, 0.156 T.

Effect of Reduction Temperature on the Concentration of Ni and Fe Beneficiation

Experimental conditions: $Na_2S_2O_3$ addition, 20 wt%; reduction time, 90 min; flow rate of H_2/N_2, 27 L/(min·kg); gas volume fraction of H_2, 45 vol%; grinding fineness, 85 wt% passing 0.074 mm; magnetic field intensity, 0.156 T.

Figure 3 shows the evolution of the magnetic products as a function of the reduction temperature. **Figure 3A** shows that the grade and recovery of Ni in the magnetic products increased with increasing reduction temperature, which increased from 1.53 to 45.77% at 600°C to 9.97% and 99.24% at 1100°C, respectively. Under the low reduction temperatures (below 700°C), the increase in the nickel grade and recovery of the concentrates were still not evident, which may have been because the promoting reaction between $Na_2S_2O_3$ and laterite was not apparent. Nevertheless, when the temperature exceeded 800°C, the nickel grade and recovery were sharply improved. Thus, 800°C could be considered to be an inflection point. At 800°C, recrystallization of the amorphous silicate occurred (Lu et al., 2013). The restructuring of magnesium silicate promoted the reaction of silicate with $Na_2S_2O_3$, and thus, the exchange between nickel and Na^+ was accelerated. Finally, the nickel grade and recovery of concentrate ore were improved. The nickel grade and recovery could be remarkably increased by increasing the temperature after the inflection point. When the reaction temperature was 1100°C, the nickel grade and recovery reached their maximum values of 9.97 and 99.24%, respectively.

Figure 3B shows that the grade of iron was only slightly changed with the increase in temperature, while the recovery rate of iron firstly increased before 900°C and then decreased as the reduction temperature increased, which may be due to the gradually increased reduction degree of iron oxides as the temperature increased. When the temperature was further increased, $Na_2S_2O_3$ could interact with the iron phase to form FeS substances (as shown in **Figure 8**) and eliminate impurities, and hence, the selective nickel-iron recovery rate could be achieved. Since these results were slightly higher than those obtained at the reaction temperature of 1000°C (9.67% of nickel grade and 98.32% of nickel recovery), the reaction temperature of 1000°C was selected for the following experiments.

Effect of Reducing Time on Concentration of Ni and Fe Beneficiation

The magnetic separation results of the prepared ore (PO) reduced at 1,000°C as a function of reduction time ranging from 30 to 120 min are shown in **Figure 4**. The prolonged reduction time could significantly promote the Ni recovery, whereas it could only slightly improve the nickel grade (**Figure 4A**). As the reaction time increased, the reduction degree, the nickel grade, and recovery rate of Ni increased initially. However, when the reaction exceeded a certain degree, the iron oxides were also over-reduced to metal iron, which could result in the nickel grade declining in the concentrate. **Figure 4B** shows that the grade and recovery rate of iron remained unchanged with the increase in the reduction time, which indicated that the influence of the reduction time on the grade and recovery rate of iron was negligible.

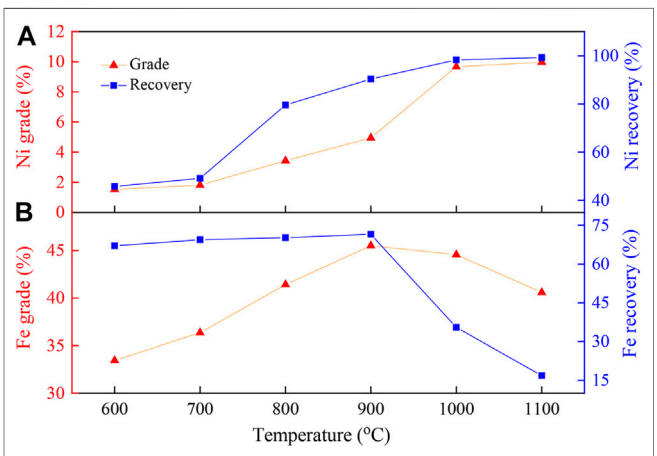

FIGURE 3 | Effect of reduction temperature on **(A)** nickel and **(B)** iron enrichment.

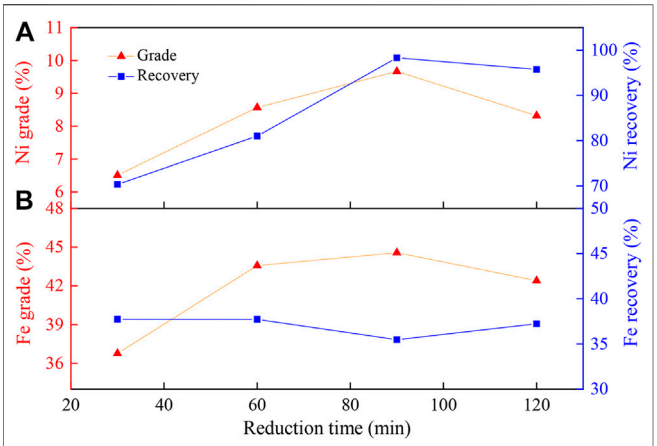

FIGURE 4 | Effect of reduction time on **(A)** nickel and **(B)** iron enrichment. Experimental conditions: $Na_2S_2O_3$ addition, 20 wt%; temperature, 1000°C; flow rate of H_2/N_2, 27 L/(min·kg); gas volume fraction of H_2, 45 vol%; grinding fineness, 85 wt% passing 0.074 mm; magnetic field intensity, 0.156 T.

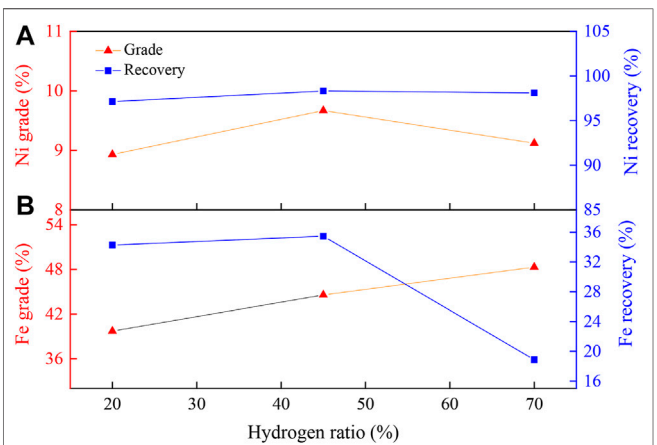

FIGURE 5 | Effect of H_2 ratio on **(A)** nickel and **(B)** iron enrichment. Experimental conditions: pre-calcination, 450°C, 60 min; temperature, 1000°C; reduction time, 90 min; flow rate of H_2/N_2, 27 L/(min kg); grinding fineness, 85 wt% passing 0.074 mm; magnetic field intensity, 0.156 T.

Effect of H_2 Ratio on Concentration of Ni and Fe Beneficiation

Figure 5 displays the effect of H_2 ratio on the nickel and iron enrichment. As shown in **Figure 5A**, with the increase in the H_2 ratio, the nickel grade increased first and then decreased, while its recovery rate remained almost unchanged. When the H_2 ratio was 45 vol%, the nickel grade and recovery reached maximum values of 9.67 and 98.32%, respectively. This was attributed to the different reduction states of the iron oxides with different H_2 ratios. With a H_2 ratio of 20 vol%, most of the iron oxides were reduced to Fe_3O_4. During the magnetic separation process, due to the strong magnetic property of Fe_3O_4, large amounts of Fe_3O_4 and Ni were magnetically separated into the concentrate, leading to decline in concentrate nickel grade. With the H_2 ratio of 70 vol%, most of the iron oxides were reduced to Fe, which would then melt with nickel to form ferronickel above 900°C (Zhu et al., 2012a), causing a high iron content in the nickel concentrate and a decreased nickel grade. At a H_2 ratio of 45 vol%, iron oxide was reduced to non-magnetic FeO, which could be discarded with the gangue component in the subsequent magnetic separation, thereby reducing the recovery of iron and improving the nickel

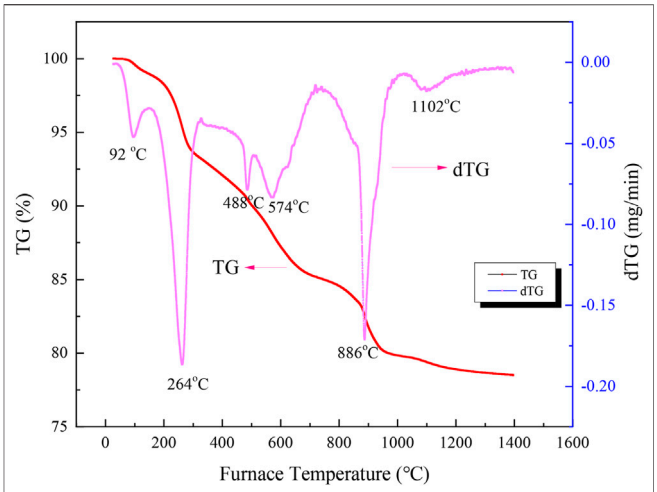

FIGURE 6 | TG-DTG curves of the $Na_2S_2O_3$/laterite blend.

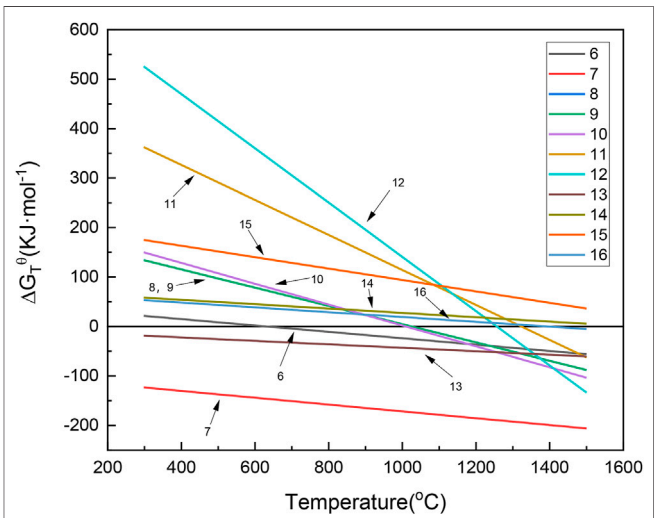

FIGURE 7 | Change of the Gibbs free energy with and without the addition of sodium thiosulfate under an H_2 atmosphere. (6): $Mg_3(OH)_4Si_2O_5 = Mg_2SiO_4+MgSiO_3+2H_2O(g)$; (7): $Al_2(OH)_4Si_2O_5 = Al_2O_3{\cdot}2SiO_2+2H_2O(g)$; (8): $Na_2S_2O_3 = S(g) + Na_2SO_3$; (9): $4Na_2SO_3 = 3Na_2SO_4+Na_2S$; (10): $H_2(g)+2(Mg,Ni)SiO_4+Na_2SO_4 = Na_2Mg_2Si_2O_7+2NiO + SO_2(g)+H_2O(g)$; (11): $H_2(g) +Ni_2SiO_4 + Na_2SO_4 = Na_2SiO_3 + 2NiO + SO_2(g) + H_2O(g)$; (12): $H_2(g) +2Ni_2SiO_4 + Na_2SO_4 = Na_2Si_2O_5 + 4NiO + SO_2(g) + H_2O(g)$; (13): $2H_2(g) +Ni_2SiO_4 + 2Na_2SO_4 = Na_4SiO_4 + 2NiO + 2SO_2(g) + 2H_2O(g)$; (14): $3H_2(g) +2Ni_2SiO_4+3Na_2SO_4 = Na_6Si_2O_7 + 4NiO +3SO_2(g) +3H_2O(g)$; (15): $H_2(g)+NiO = Ni + H_2O(g)$; (16): $H_2(g) +Ni_2SiO_4 = NiSiO_3+Ni + H_2O(g)$.

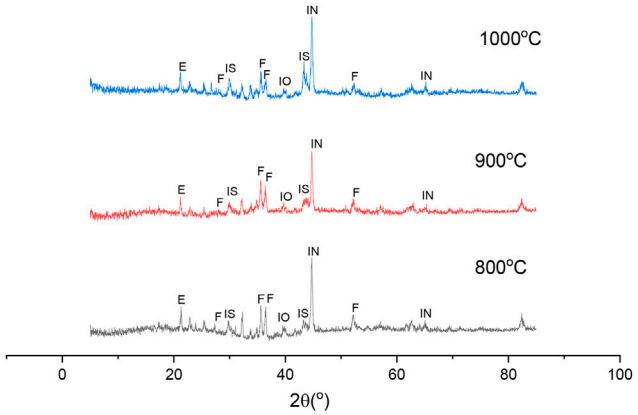

FIGURE 8 | XRD patterns of roasted ores under different reduction roasting temperatures: (IN) Iron-Nickel, (IS) FeS, (F) $Na_2Mg_2Si_2O_8$ Forsterit, (E) Enstatite, (IO) Iron Oxide.

grade. According to **Figure 5B**, as the proportion of hydrogen increased, the iron grade did not change significantly, while the iron recovery rate showed a peak value at 45 vol%. The iron recovery rate could be enhanced due to the improved reduction degree of iron oxides with increasing H_2 ratio. When the H_2 ratio was further increased, the reduction degree of $Na_2S_2O_3$ and iron was further increased, forming FeS, which affected the recovery rate of ferric oxygen. Therefore, a 45 vol% of H_2 ratio was selected as the optimal hydrogen ratio.

Reduction Mechanism of Nickel Laterite Ore Improved by Sodium Thiosulfate

Behavior of Pyrolysis Characteristics of Laterite With $Na_2S_2O_3$

To clarify the reaction mechanism of $Na_2S_2O_3$ on the laterite nickel ore reduction, the thermal characteristics of the laterite blended with 20 wt% $Na_2S_2O_3$ were investigated by TG-DTG, as shown in **Figure 6**.

From **Figure 6**, five steps can be found in the net weight loss curve of mixture during the heating process. The first step occurred between room temperature to 141°C, with a weight loss of 1.03%, which could be due to the free water removal of laterite nickel ore and $Na_2S_2O_3$ (Mcamish and Johnston, 1976). The second step occurred between 152 to 298°C, and 4.87% weight loss was observed during the process, which was attributed to the bound water loss from $Na_2S_2O_3{\cdot}5H_2O$, as follows:

$$Na_2S_2O_3 \cdot 5H_2O = Na_2S_2O_3 + 5H_2O \quad (4)$$

In the temperature range from 416 to 503 °C, 1.84% of the mass was lost, which may have been attributed to the dehydroxylation of goethite-type hematite in laterite nickel ore, shown as follows (Lu et al., 2013).

$$2FeO(OH) = Fe_2O_3 + H_2O(g) \quad (5)$$

The fourth stage showed a 4.24% net weight loss from 523 to 704°C, which was assigned to the decomposition of $Na_2S_2O_3$ to S and Na_2SO_3 at 488°C and the dehydroxylation of serpentine and kaolinite in the laterite

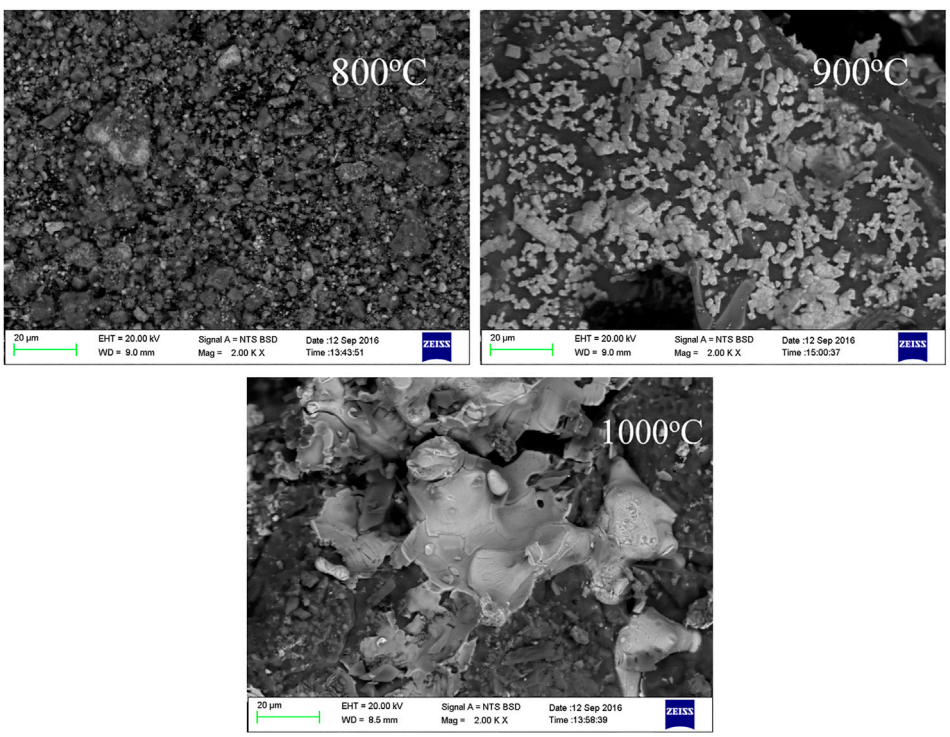

FIGURE 9 | SEM images of roasted laterite ores with $Na_2S_2O_3$ under different roasting temperatures.

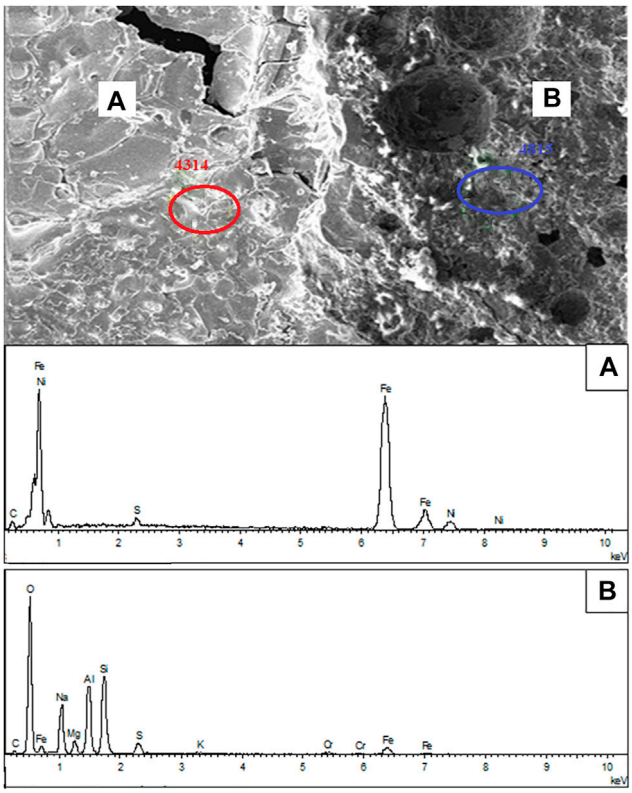

FIGURE 10 | SEM-EDS analysis of the calcined product of laterite/$Na_2S_2O_3$ blends: **(A)** bright area and **(B)** gray area.

nickel ore with a peak positioned at 574°C (Lu et al., 2013). The sulphidation of a nickeliferous lateritic ore was studied at temperatures between 450 and 1100°C, and the nickel could be selectively sulfidized to form a nickel-iron sulfide (Harris et al., 2011; Harris et al., 2013; Ding et al., 2020). These processes can be described by the following reactions:

$$Mg_3(OH)_4Si_2O_5 = Mg_2SiO_4 + MgSiO_3 + 2H_2O(g) \quad (6)$$

$$Al_2(OH)_4Si_2O_5 = Al_2O_3 \cdot 2SiO_2 + 2H_2O(g) \quad (7)$$

$$Na_2S_2O_3 = S(g) + Na_2SO_3 \quad (8)$$

The final step occurred from 759 to 1042°C with a net weight loss of 5.26%. In this stage, the disproportionation of Na_2SO_3 to Na_2SO_4 and Na_2S occurred as follows:

$$4Na_2SO_3 = 3Na_2SO_4 + Na_2S \quad (9)$$

The recrystallization of magnesia-nickel silicate by the sodium salts also occurred after H_2 introduction, which could transform the nickel in the silicate to form NiO, as **Equation 8** (Li et al., 2012).

$$H_2(g) + 2(Mg, Ni)SiO_4 + Na_2SO_4 = Na_2Mg_2Si_2O_7 + 2NiO + SO_2(g) + H_2O(g) \quad (10)$$

$$H_2(g) + Ni_2SiO_4 + Na_2SO_4 = Na_2SiO_3 + 2NiO + SO_2(g) + H_2O(g) \quad (11)$$

$$H_2(g) + 2Ni_2SiO_4 + Na_2SO_4 = Na_2Si_2O_5 + 4NiO + SO_2(g) + H_2O(g) \quad (12)$$

$$2H_2(g) + Ni_2SiO_4 + 2Na_2SO_4 = Na_4SiO_4 + 2NiO + 2SO_2(g) + 2H_2O(g) \quad (13)$$

$$3H_2(g) + 2Ni_2SiO_4 + 3Na_2SO_4 = Na_6Si_2O_7 + 4NiO + 3SO_2(g) + 3H_2O(g) \quad (14)$$

$$H_2(g) + NiO = Ni + H_2O(g) \quad (15)$$

$$H_2(g) + Ni_2SiO_4 = NiSiO_3 + Ni + H_2O(g) \quad (16)$$

$$3H_2(g) + 2Ni_2SiO_4 = NiSi_2O_5 + 3Ni + 3H_2O(g) \quad (17)$$

$$H_2(g) + 2Ni_2SiO_4 = Ni_3Si_2O_7 + Ni + H_2O(g) \quad (18)$$

Figure 7 shows the Gibbs free energy of laterite ore reduction by H_2 with and without the addition of sodium thiosulfate. The decomposition of $Na_2S_2O_3$ to S and Na_2SO_3 occurred at about 680 K, and Na_2SO_3 could decompose to Na_2SO_4 and Na_2S at 298 K. **Eqs 8–12** are reduction reactions of laterite nickel ore with sodium sulfate under a H_2 atmosphere. According to **Supplementary Table S1 and S2**, thermodynamic data suggests that the above reactions could occur at approximately 1000 K. However, laterite nickel ore cannot be reduced by H_2 without sodium sulfate, corresponding to **Eqs 13–16**. Therefore, laterite nickel ore can be effectively reduced by H_2 with the help of sodium thiosulfate.

Phase Transformations of Nickel Laterite Ore During Reduction

To reveal the effect of sodium thiosulfate on the reduction and beneficiation of nickel laterite, the XRD patterns of the reduction residue of laterite ore were analyzed, as shown in **Figure 8**. With the increase in the reduction temperature, the intensity of the nickel-iron increased gradually with the consumption of iron oxide, which indicates that the higher temperature was beneficial for the accumulation of nickel-iron. This accumulation may have been due to the formation of the low melting eutectic phase of the FeS-Fe system, which could improve the mobility of the reaction system. Therefore, the transfer between the phases was accelerated (Li et al., 2012; Jiang et al., 2013; Lu et al., 2013). The peak of $Na_2Mg_2Si_2O_8$ increased gradually with the increase in the reaction temperature, which indicated that the heating could promote the activity of the sodium salts and accelerated the reaction between the sodium salts and nickel-magnesium. Meanwhile, the nickel release and reduction were also promoted, thereby improving the grade of the nickel concentrate (de Alvarenga Oliveira et al., 2019).

Melting and Particle Growth of Ni-Fe During the Reduction

Figure 9 presents the micrographs of the reduced PO at different temperatures for 90 min in the presence of sodium thiosulfate. The metallic particle grains of the nickel laterite grew larger at higher temperatures. Moreover, the metallic particle grains of the nickel laterite with sodium thiosulfate were much larger than those without sodium thiosulfate, which was consistent with previous results (Ilyas and Koike, 2012). With the increase in the calcination temperature from 800 to 1000°C, the nickel-iron

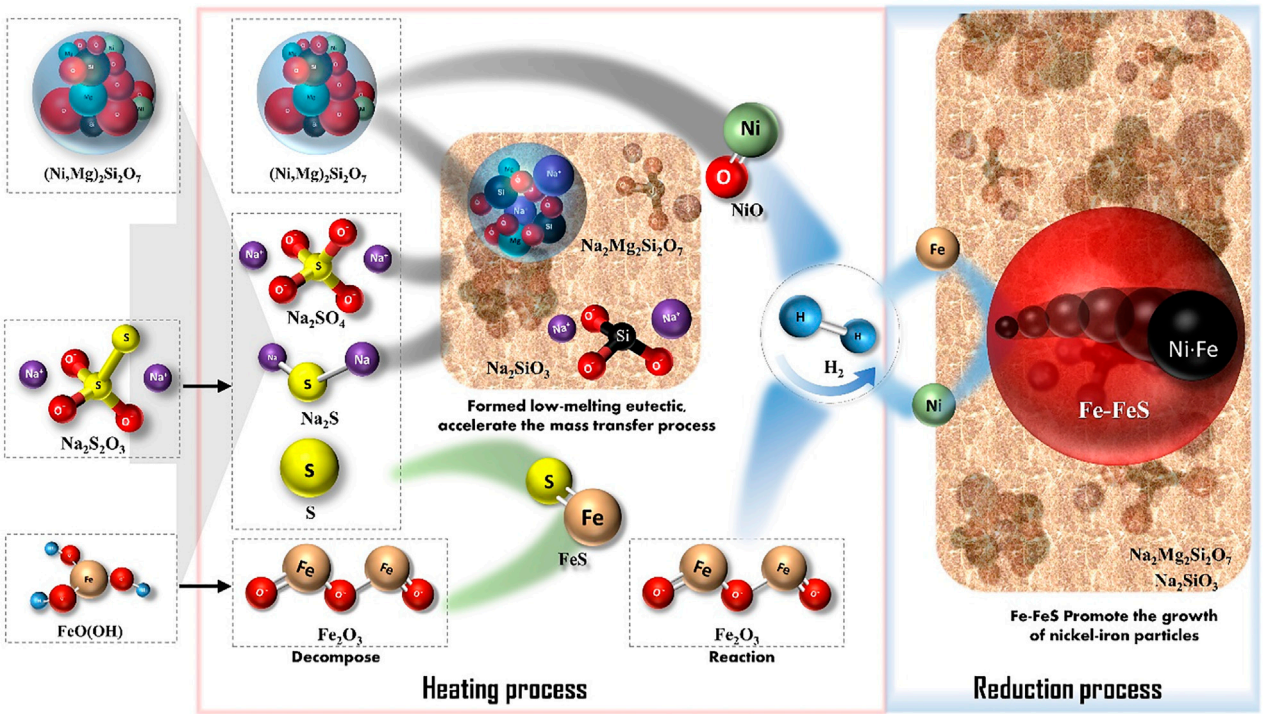

FIGURE 11 | Hydrogen-thermal reduction mechanism of laterite ore enhanced by $Na_2S_2O_3$.

particles dispersed in the minerals gradually accumulated and grew, and finally formed a lamellar eutectic. This may be due to the low-melting-point eutectic of Fe-FeS formed in the reduction process with the elemental sulfur produced by the decomposition of $Na_2S_2O_3$ (Mcamish and Johnston, 1976). However, Na_2O, which was formed by the decomposition of $Na_2S_2O_3$, replaced the nickel wrapped in magnesium-containing silicate minerals and formed low-melting-point substances (Na_2SiO_3) (Li et al., 2012). The low melting point eutectic could directionally aggregate the nickel-iron particles on the solid surface. Therefore, it was beneficial for the magnetic separation process of the Ni-Fe enrichment.

To explore the inherent nature of the aggregation and growth of nickel-iron particles, the reduction residue under 1,000°C with 20 wt% $Na_2S_2O_3$ was analyzed by EDS, as shown in **Figure 10**. Two distinct zones-the bright area and the gray area-were evident on the surface. As indicated by the EDS result, the bright areas were mainly composed of Ni and Fe with small amount of S, which suggests the accumulation of nickel-iron particles. However, the gray areas mainly contained Si, Al, Na, Mg, O and small amounts of Fe, indicating the presence of gangue, such as magnesium and sodium silicate minerals.

The possible reasons for the Ni grade and recovery improvement by $Na_2S_2O_3$ are as following. On the one hand, the $Na_2S_2O_3$ could decompose to S, which could participate in the formation of Fe-FeS as the low point eutectic phase (Lu et al., 2013). With the help of this eutectic phase, the nickel-iron particles could be directionally accumulated and then benefit the subsequent magnetic separation progress. On the other hand, the $Na_2S_2O_3$ could also provide Na_2O (alkali metal salt), which could replace the nickel wrapped in magnesium-containing silicate mineral. Therefore, the recovery rate of the nickel concentration was improved.

Mechanism of Sodium Thiosulfate in Promoting Reduction of Laterite Ore by H_2

The mechanism of $Na_2S_2O_3$ for promoting reduction of the laterite ore is shown in **Figure 11**. $Na_2S_2O_3$ played multiple role in the hydrogen reduction as sulfur and alkali metal salt providers. The reaction mechanism is described as follows: 1) During the heating step, $Na_2S_2O_3$ decomposed to S, Na_2SO_4, and Na_2S. 2) S then reacted with iron oxides, which decomposed from goethite in the laterite nickel ore to form FeS; Na_2SO_4 and Na_2S destroyed the structures of the nickel-bearing silicate minerals at higher temperatures, releasing the nickel wrapped in magnesium-containing silicate minerals and forming a low-melting-point eutectic phase ($Na_2Mg_2Si_2O_8$). 3) During the H_2 reduction stage, NiO and iron oxide were reduced to their metal phases, after which the fine nickel and iron particles directionally aggregated and grew with the help of FeS-Fe (low melting point eutectic phase). 4) As large amounts of sodium silicate entered the liquid phase, element migration was enhanced and hence the reduction and growth process of the Fe-Ni were accelerated.

CONCLUSION

In summary, sodium thiosulfate was firstly applied to enhance the reduction of laterite ore by H_2. The maximum values of 9.97 and 99.24% were achieved for the nickel grade and recovery, respectively, at 1,000°C with the addition of 20 wt% $Na_2S_2O_3$. $Na_2S_2O_3$ played multiple roles as sulfur and alkali metal salt providers simultaneously to improve the reduction. A possible mechanism of sodium thiosulfate in promoting the reduction of laterite ore can be concluded as follows: $Na_2S_2O_3$ was firstly decomposed to S, Na_2SO_4, and Na_2S. The alkali metal salts then destroyed the structures of nickel-bearing silicate minerals to liberate nickel as nickel oxide, while S reacted with Fe to form a low melting point eutectic phase of FeS-Fe. Fine nickel and iron particles were directionally aggregated and grew due to the capillary forces of the FeS-Fe system under H_2 reduction. In addition, the massive formation of sodium silicate in the liquid phase reduced the reaction temperature by enhancing the element migration ability simultaneously. Hence, the reduction and growth process of the Fe-Ni were accelerated.

DATA AVAILABILITY STATEMENT

The original contributions presented in the study are included in the article/**Supplementary Material**, further inquiries can be directed to the corresponding authors.

AUTHOR CONTRIBUTIONS

SL contributed to the conception of the study. CY contributed significantly to analysis and manuscript preparation; SY performed the data analyses and wrote the manuscript; ZY helped perform the analysis with constructive discussions. JL and ZW drew diagrams and tables and optimized them. KY and XL have modified the format of the article.

FUNDING

This study was supported by National Natural Science Foundation of China (21878210), Shanxi Province patent promotion grant program (20200719), Scientific and Technological Innovation Programs of Higher Education Institutions in Shanxi (2019L0313), "1331 project" research center in Shanxi and sponsored by Mettler Toledo, Taiyuan Green Coke Energy Co., Ltd. (China).

SUPPLEMENTARY MATERIAL

The Supplementary Material for this article can be found online at: https://www.frontiersin.org/articles/10.3389/fchem.2021.704012/full#supplementary-material

REFERENCES

de Alvarenga Oliveira, V., de Jesus Taveira Lana, R., da Silva Coelho, H. C., Brigolini, G. J. S., and dos Santos, C. G. (2020). Kinetic Studies of the Reduction of Limonitic Nickel Ore by Hydrogen. *Metall. Mater. Trans. B* 51, 1418–1431. doi:10.1007/s11663-020-01841-9

de Alvarenga Oliveira, V., dos Santos, C. G., and de Albuquerque Brocchi, E. (2019). Assessing the Influence of NaCl on the Reduction of a Siliceous Laterite Nickel Ore under Caron Process Conditions. *Metall. Materi Trans. B* 50, 1309–1321. doi:10.1007/s11663-019-01552-w

Ding, A., Zhao, Y., Yan, Z., Bai, L., Yang, H., Liang, H., et al. (2020). Co-application of Energy Uncoupling and Ultrafiltration in Sludge Treatment: Evaluations of Sludge Reduction, Supernatant Recovery and Membrane Fouling Control. *Front. Environ. Sci. Eng.* 14, 13–52. doi:10.1007/s11783-020-1238-9

Harris, C. T., Peacey, J. G., and Pickles, C. A. (2011). Selective Sulphidation of a Nickeliferous Lateritic Ore. *Miner. Eng.* 24, 651–660. doi:10.1016/j.mineng.2010.10.008

Harris, C. T., Peacey, J. G., and Pickles, C. A. (2013). Selective Sulphidation and Flotation of Nickel from a Nickeliferous Laterite Ore. *Miner. Eng.* 54, 21–31. doi:10.1016/j.mineng.2013.02.016

Hidayat, T., Rhamdhani, M. A., Jak, E., and Hayes, P. C. (2008). The Characterization of Nickel Metal Pore Structures and the Measurement of Intrinsic Reaction Rate during the Reduction of Nickel Oxide in H2-N2 and H2-H2O Atmospheres. *Miner. Eng.* 21, 157–166. doi:10.1016/j.mineng.2007.09.004

Hu, D., Xu, H., Yi, Z., Chen, Z., Ye, C., Wu, Z., et al. (2019). Green CO_2-Assisted Synthesis of Mono- and Bimetallic Pd/Pt Nanoparticles on Porous Carbon Fabricated from Sorghum for Highly Selective Hydrogenation of Furfural. *ACS Sustain. Chem. Eng.* 7, 15339–15345. doi:10.1021/acssuschemeng.9b02665

Ilyas, A., and Koike, K. (2012). Geostatistical Modeling of Ore Grade Distribution from Geomorphic Characterization in a Laterite Nickel Deposit. *Nat. Resour. Res.* 21, 177–191. doi:10.1007/s11053-012-9170-8

Jiang, M., Sun, T., Liu, Z., Kou, J., Liu, N., and Zhang, S. (2013). Mechanism of Sodium Sulfate in Promoting Selective Reduction of Nickel Laterite Ore during Reduction Roasting Process. *Int. J. Mineral Process.* 123, 32–38. doi:10.1016/j.minpro.2013.04.005

Katzagiannakis, N., Alevizos, G., Stamboliadis, E., Stratakis, A., and Petrakis, E. (2014). Mineralogical Investigation and Washability Treatment of the Nickeliferous Lateritic Deposit of Nome (Albania). *Geomaterials* 04, 105–115. doi:10.4236/gm.2014.43011

Khataee, A., Salahpour, F., Fathinia, M., Seyyedi, B., and Vahid, B. (2015). Iron Rich Laterite Soil with Mesoporous Structure for Heterogeneous Fenton-like Degradation of an Azo Dye under Visible Light. *J. Ind. Eng. Chem.* 26, 129–135. doi:10.1016/j.jiec.2014.11.024

Kim, J., Dodbiba, G., Tanno, H., Okaya, K., Matsuo, S., and Fujita, T. (2010). Calcination of Low-Grade Laterite for Concentration of Ni by Magnetic Separation. *Minerals Eng.* 23, 282–288. doi:10.1016/j.mineng.2010.01.005

Li, G., Shi, T., Rao, M., Jiang, T., and Zhang, Y. (2012). Beneficiation of Nickeliferous Laterite by Reduction Roasting in the Presence of Sodium Sulfate. *Miner. Eng.* 32, 19–26. doi:10.1016/j.mineng.2012.03.012

Lu, J., Liu, S., Shangguan, J., Du, W., Pan, F., and Yang, S. (2013). The Effect of Sodium Sulphate on the Hydrogen Reduction Process of Nickel Laterite Ore. *Miner. Eng.* 49, 154–164. doi:10.1016/j.mineng.2013.05.023

Mcamish, L. H., and Johnston, F. J. (1976). Sulfur Exchange and Decomposition Kinetics in Solid Na2S2O3. *J. Inorg. Nucl. Chem.* 38, 537–540. doi:10.1016/0022-1902(76)80299-0

Moskalyk, R. R., and Alfantazi, A. M. (2002). Nickel Laterite Processing and Electrowinning Practice. *Miner. Eng.* 15, 593–605. doi:10.1016/s0892-6875(02)00083-3

Quast, K., Connor, J. N., Skinner, W., Robinson, D. J., and Addai-Mensah, J. (2015). Preconcentration Strategies in the Processing of Nickel Laterite Ores Part 1: Literature Review. *Miner. Eng.* 79, 261–268. doi:10.1016/j.mineng.2015.03.017

Quast, K., Connor, J. N., Skinner, W., Robinson, D. J., Li, J., and Addai-Mensah, J. (2015). Preconcentration Strategies in the Processing of Nickel Laterite Ores Part 2: Laboratory Experiments. *Miner. Eng.* 79, 269–278. doi:10.1016/j.mineng.2015.03.016

Sudagar, J., Lian, J., and Sha, W. (2013). Electroless Nickel, alloy, Composite and Nano Coatings - A Critical Review. *J. Alloys Compd.* 571, 183–204. doi:10.1016/j.jallcom.2013.03.107

Valente, A., Iribarren, D., and Dufour, J. (2020). Prospective Carbon Footprint Comparison of Hydrogen Options. *Sci. Total Environ.* 728, 138212. doi:10.1016/j.scitotenv.2020.138212

Valix, M., and Cheung, W. H. (2002). Effect of Sulfur on the mineral Phases of Laterite Ores at High Temperature Reduction. *Miner. Eng.* 15, 523–530. doi:10.1016/s0892-6875(02)00069-9

Zeissink, H. E. (1969). The Mineralogy and Geochemistry of a Nickeliferous Laterite Profile (Greenvale, Queensland, Australia). *Mineralium Deposita* 4, 132–152. doi:10.1007/bf00208049

Zhang, M., Liu, Y., Liu, B., Chen, Z., Xu, H., and Yan, K. (2020). Trimetallic NiCoFe-Layered Double Hydroxides Nanosheets Efficient for Oxygen Evolution and Highly Selective Oxidation of Biomass-Derived 5-Hydroxymethylfurfural. *ACS Catal.* 10, 5179–5189. doi:10.1021/acscatal.0c00007

Zhu, D.-Q., Cui, Y., Hapugoda, S., Vining, K., and Pan, J. (2012). Mineralogy and crystal Chemistry of a Low Grade Nickel Laterite Ore. *Trans. Nonferrous Met. Soc. China* 22, 907–916. doi:10.1016/s1003-6326(11)61264-8

Zhu, D. Q., Cui, Y., Vining, K., Hapugoda, S., Douglas, J., Pan, J., et al. (2012). Upgrading Low Nickel Content Laterite Ores Using Selective Reduction Followed by Magnetic Separation. *Int. J. Miner. Process.* 106-109, 1–7. doi:10.1016/j.minpro.2012.01.003

Conflict of Interest: Author JL was employed by the company Taiyuan Green Coke Energy Co. Ltd.

The remaining authors declare that the research was conducted in the absence of any commercial or financial relationships that could be construed as a potential conflict of interest.